Monthly Notices
of the
ROYAL ASTRONOMICAL SOCIETY

MNRAS **428,** 502–517 (2013) doi:10.1093/mnras/sts038

Five old open clusters more in the outer Galactic disc

Giovanni Carraro,[1,2]★ Yuri Beletsky[3] and Gianni Marconi[1]

[1]*European Southern Observatory, Alonso de Cordova 3107 Vitacura, Santiago de Chile, Chile*
[2]*Dipartmento di Astronomia, Universitá di Padova, Vicolo Osservatorio 3, I-35122 Padova, Italy*
[3]*Las Campanas Observatory, Carnegie Institution of Washington, Colina el Pino, Casilla 601 La Serena, Chile*

Accepted 2012 September 19. Received 2012 September 7; in original form 2012 April 30

ABSTRACT

New photometric material is presented for six outer disc supposedly old, Galactic star clusters: Berkeley 76, Haffner 4, Ruprecht 10, Haffner 7, Haffner 11 and Haffner 15, which are projected against the rich and complex Canis Major overdensity at $225^\circ \leq l \leq 248^\circ$, $-7^\circ \leq b \leq -2^\circ$. This CCD data set, in the *UBVI* passbands, is used to derive their fundamental parameters, in particular age and distance. Four of the program clusters turn out to be older than 1 Gyr. This fact makes them ideal targets for future spectroscopic campaigns aiming at deriving their metal abundances. This, in turn, contributes to increase the number of well-studied outer disc old open clusters. Only Haffner 15, previously considered an old cluster, is found to be a young, significantly reddened cluster, member of the Perseus arm in the third Galactic quadrant. As for Haffner 4, we suggest an age of about half a Gyr. The most interesting result we found is that Berkeley 76 is probably located at more than 17 kpc from the Galactic centre, and therefore is among the most peripherical old open clusters so far detected. Besides, for Ruprecht 10 and Haffner 7, which were never studied before, we propose ages larger than 1 Gyr.

All the old clusters of this sample are scarcely populated and show evidence of tidal interaction with the Milky Way, and are therefore most probably in advanced stages of dynamical dissolution.

Key words: open clusters and associations: general – open clusters and associations: individual: Berkeley 76, Haffner 4, Ruprecht 10, Haffner 7, Haffner 11, Haffner 15.

1 INTRODUCTION

The structure and evolution of the outer Galactic disc have been the subject of intense investigation in the last years (Frinchaboy et al. 2004; Momany et al. 2006; Carraro et al. 2007a, 2010). This is because the outer disc in the anticentre direction is less dominated by confusion than other Galactic directions, a fact which renders it easier to describe its structure and to search for signatures of ongoing or past accretion events. The latter consist of the Monoceros Ring (Chou et al. 2010, and references therein), and the Canis Major overdensity (Momany et al. 2006). However, both these structures are now considered by most researchers to be caused by the warped and flared Galactic disc (López-Corredoira et al. 2007, 2012; Carraro, Moitinho & Vázquez 2008).

Among the various tracers routinely used to probe the outer disc, Galactic open clusters offer the advantage that it is relatively easy to obtain estimates of their ages and distances, and that they are ubiquitous in the outer disc. This is a valid statement for both old and young open clusters, since the deficiency of old open clusters is most visible in the inner disc, due to the more difficult environment which prevents a cluster to survive for a long time.

In this paper we derive basic parameters of six anticentre clusters, located in the third quadrant of the Galactic disc: Berkeley 76, Haffner 4, Ruprecht 10, Haffner 7, Haffner 11 and Haffner 15 (see Table 1, where for each cluster we report Equatorial and Galactic coordinates, together with an estimate of the reddening at infinity in their direction). The rich fields they are projected against have been already studied in detail in Vázquez et al. (2008), where we highlight the properties of the conspicuous young populations we detected and use it to probe the spiral structure in that quadrant. The analysis of the clusters we performed in that paper was quite preliminary, and for this reason in this paper we are going to present the data, show the photometric diagrams, provide an extensive analysis of them, and propose updated estimates of distance and age for these clusters. In a few cases, these estimates are given for the very first time.

Interestingly enough, we anticipate that these clusters turn out to be all older than 1 Gyr, except for Haffner 5, which is a young, highly obscured cluster. This constitutes quite a useful result per se,

★ E-mail: gcarraro@eso.org

Table 1. Basic parameters of the clusters under investigation. Coordinates are for J2000.0. We list also equatorial coordinates in degrees (columns 4 and 5), to help the reader to look at Figs 1 and 3. The last column reports the expected reddening along the line of sight all the way to infinity according to Schlegel, Finkbeiner & Davis (1998) maps.

Name	RA (hh:mm:ss)	Dec. (°: ′: ″)	RA (°)	Dec. (°)	l (°)	b (°)	$E(B-V)_\infty$ (mag)
Berkeley 76	07:06:24	−11:37:00	106.60	−11.62	225.099	−1.998	0.740
Haffner 4	07:06:12	−14:59:00	106.55	−14.98	227.940	−3.586	0.721
Ruprecht 10	07:06:25	−20:05:00	106.60	−20.08	232.553	−5.854	0.645
Haffner 7	07:22:55	−29:30:00	110.73	−29.50	242.673	−6.804	0.270
Haffner 11	07:35:25	−27:43:00	113.85	−27.72	242.395	−3.544	0.824
Haffner 15	07:45:32	−32:51:00	116.38	−32.85	247.952	−4.158	1.558

since it contributes to improve the statistics of old clusters in the Galactic disc outer regions and therefore can help to provide tighter constraints for chemical evolution models aiming at recovering the chemical history and assembly of the outer disc (Carraro et al. 2007a).

The paper is organized as follows. In Section 1 we present the data, the observation strategy, and the extraction and calibration of the photometry. In the same section, details are provided on the astrometry, completeness and star count analysis. A summary of the information available in the literature for these clusters is presented in Section 2, while Section 3 introduces the basic diagrams we use to extract clusters' fundamental parameters. Finally, Section 4 summarizes the results and discusses their implications.

1.1 Observations and data reduction

The targets were observed with the Y4KCAM camera attached to the Cerro Tololo Inter-American Observatory (CTIO) 1-m telescope, operated by the Small and Moderate Aperture Research Telescope System (SMARTS) consortium[1] during an observation run in 2005 November–December. This camera is equipped with an Semiconductor Technology Associates (STA) 4064 × 4064 CCD[2] with 15-μm pixel, yielding a scale of 0.289 arcsec pixel^{-1} and a field of view (FOV) of 20 × 20 arcmin^2 at the Cassegrain focus of the CTIO 1-m telescope. The CCD was operated without binning, at a nominal gain of 1.44 e$^-$ ADU^{-1}, implying a readout noise of 7 e$^-$ per quadrant (this detector is read by means of four different amplifiers).

In Table 2 we present the log of our *UBVI* observations, while in Fig. 1 we show astrometrized images, resulting from montaging all the available exposures and filters. All observations were carried out in photometric, good-seeing (always less than 1.2 arcsec), conditions. Our *UBVI* instrumental photometric system was defined by the use of a standard broad-band Kitt Peak $UBVI_{kc}$ set of filters.[3] To determine the transformation from our instrumental system to the standard Johnson–Kron–Cousins system, and to correct for extinction, we observed stars in Landolt's areas Rubin 149, SA 95, TPhe, PG 0231 (Landolt 1992) multiple times and with different airmasses ranging from ∼1.03 to ∼2.0, and covering quite a large colour range of $-0.3 \leq (B-V) \leq 1.7$ mag.

Table 2. *UBVI* photometric observations of star clusters.

Target	Date	Filter	Exposure (s)	Airmass
Haffner 15	2005 November 30	*U*	60, 1000	1.00−1.02
		B	30, 800	1.00−1.01
		V	15, 400	1.00−1.01
		I	15, 400	1.00−1.01
Haffner 4	2005 December 1	*U*	30, 1200	1.00−1.03
		B	20, 900	1.00−1.06
		V	15, 600	1.00−1.05
		I	15, 600	1.00−1.04
Haffner 11	2005 December 1	*U*	30, 1200	1.00−1.05
		B	20, 900	1.00−1.05
		V	15, 600	1.00−1.05
		I	15, 600	1.00−1.03
Berkeley 76	2005 December 2	*U*	30, 1200	1.05−1.08
		B	20, 900	1.06−1.09
		V	15, 600	1.07−1.08
		I	15, 60	1.06−1.09
Ruprecht 10	2005 December 3	*U*	30, 1200	1.05−1.14
		B	20, 720	1.06−1.17
		V	10, 30, 540	1.07−1.15
		I	10, 540	1.06−1.14
Haffner 7	2005 December 3	*U*	30, 1200	1.00−1.02
		B	20, 900	1.00−1.02
		V	15, 600	1.00−1.01
		I	15, 300	1.00−1.01

1.2 Photometric reductions

Basic calibration of the CCD frames was done using IRAF[4] package CCDRED. For this purpose, zero exposure frames and twilight sky flats were taken every night. Photometry was then performed using the DAOPHOT/ALLSTAR stand-alone packages. Instrumental magnitudes were extracted following the point spread function (PSF) method (Stetson 1987). A quadratic, spatially variable, master PSF (PENNY function) was adopted, because of the large FOV of the two detectors. Aperture corrections were then determined in each image by performing aperture photometry of a suitable number (typically 10–20) of bright, isolated, stars in the field. Five different apertures were used, going from the small aperture used for clusters' frame reduction (4–7 pixel, depending on the cluster) to the large one used for standard stars (14 pixel). A growth curve was then built up to estimate the correction. These total corrections were

[1] http://http://www.astro.yale.edu/smarts
[2] http://www.astronomy.ohio-state.edu/Y4KCam/detector.html
[3] http://www.astronomy.ohio-state.edu/Y4KCam/ filters.html

[4] IRAF is distributed by the National Optical Astronomy Observatory, which is operated by the Association of Universities for Research in Astronomy, Inc., under cooperative agreement with the National Science Foundation.

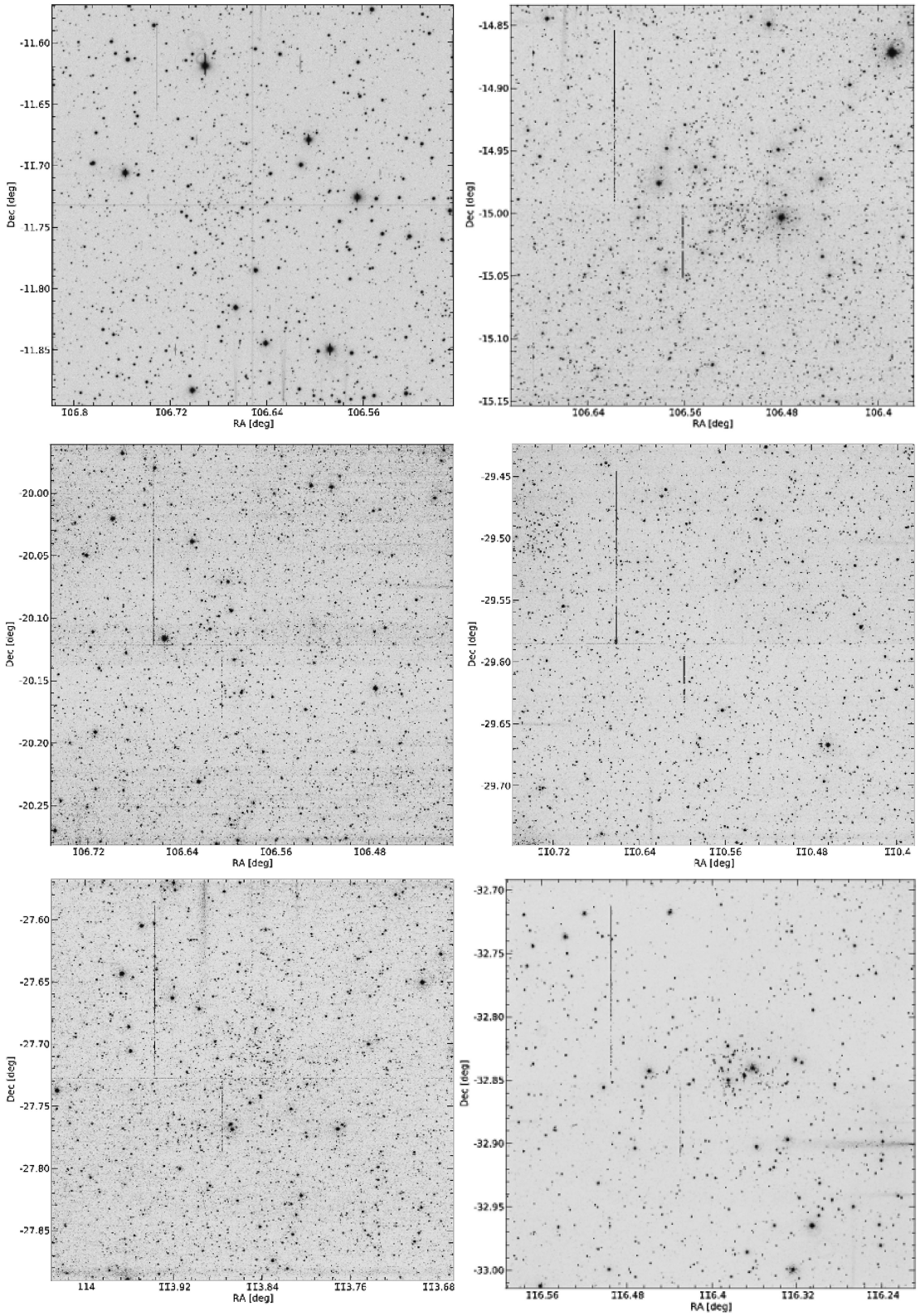

Figure 1. Montages of all CTIO CCD frames for the clusters under study. Top row (from left to right): Berkeley 76 and Haffner 4; middle row (from left to right): Ruprecht 10 and Haffner 7; bottom row (from left to right): Haffner 11 and Haffner 15.

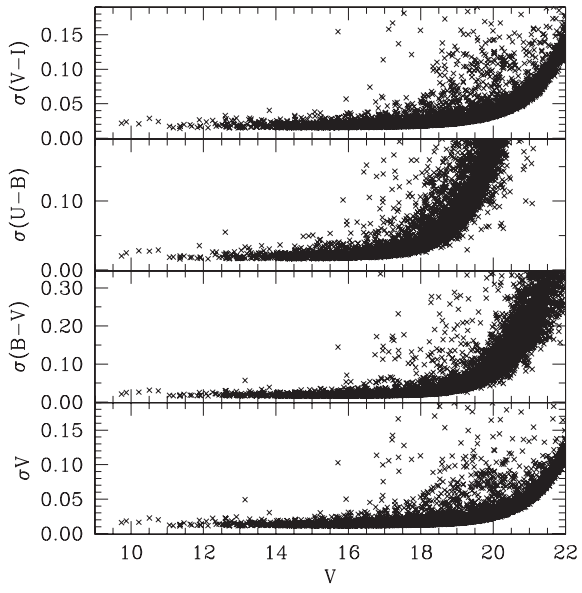

Figure 2. Trend of photometric in V, $B-V$, $U-B$ and $V-I$ as a function of V.

found to vary from 0.160 to 0.290 mag, depending on the filter. The PSF photometry was finally aperture corrected, filter by filter.

1.3 Photometric calibration

During the same observing run we observed the old open cluster Auner 1 (Carraro et al. 2007b), the dwarf planet Eris (Carraro et al. 2006) and three Galactic fields centred on the Canis Major overdensity (Carraro et al. 2008). In these papers we reported the photometric calibration procedure and the various colour equations, which we are not going to repeat here. The reader is referred to those papers for all the details. We only remind the reader that typical total errors combining ALLSTAR errors and calibration errors (see Patat & Carraro 2001, appendix A1, for details) are shown in Fig. 2.

1.4 Completeness and astrometry

Completeness corrections were determined by running artificial star experiments on the data. Basically, we created several artificial images by adding artificial stars to the original frames. These stars were added at random positions, and had the same colour and luminosity distribution of the true sample. To avoid generating overcrowding, in each experiment we added up to 20 per cent of the original number of stars. Depending on the frame, between 1000 and 5000 stars were added. In this way we have estimated that the completeness level of our photometry is better than 90 per cent down to V and $I = 20.5$.

Each optical catalogue was then cross-correlated with Two Micron All Sky Survey (2MASS), which resulted in a final catalogue including *UBVI* and JHK_s magnitudes. As a by-product, pixel (i.e. detector) coordinates were converted to RA and Dec. for J2000.0 equinox, thus providing 2MASS-based astrometry, useful for e.g. spectroscopic follow-up. The rms values of the residuals in the positions were 0.17 arcsec, which is about the astrometric precision of the 2MASS catalogue (0.12 arcsec; Skrutskie et al. 2006).

All the data discussed in this paper will be made available at the WEBDA[5] data base maintained by E. Paunzen in Vienna and at VizierR. A sample of the data is shown in Table 3 for the case of Haffner 4.

2 LITERATURE MATERIAL

We observed all these clusters back in 2005 and at that time no studies existed in literature on them.

However, in the following years, and before the analysis presented in this paper, various studies appeared. We summarize here the basic results of these investigations.

Hasegawa, Sakamoto & Malasan (2008) presented CCD *BVI* photometry of Berkeley 76 and Haffner 4. Their photometry is typically 3–4 mag shallower than the present study and rarely reaches $V \sim 19$ mag. They found (see their table 4) for Berkeley 76 an age of 1.6 Gyr for $Z = 0.000$ metallicity, a reddening $E(V-I) = 0.70$ and a corrected distance modulus $(m-M)_0 = 14.39$. As for Haffner 4, they found an age of 1.3 Gyr for a metallicity value of $Z = 0.008$, a reddening $E(V-I) = 0.40$ and a corrected distance modulus $(m-M)_0 = 13.24$.

Using the 2MASS catalogue, Bica & Bonatto (2005) derived estimates of the basic parameters of Haffner 11. They suggest that the cluster is 0.95 Gyr old, with a reddening $E(B-V) = 0.36$ and a corrected distance modulus $(m-M)_0 = 13.60$. This same cluster was later studied by Piatti et al. (2009) using photometry in the Washington system. These authors find significantly different results from Bica & Bonatto (2005), proposing that Haffner 11 is 0.5 Gyr old, with a reddening $E(B-V) = 0.57$ and a corrected distance modulus $(m-M)_0 = 13.90$.

Finally, Haffner 15 was targeted by Paunzen et al. (2006) in their search for peculiar stars in open clusters. In their study they report an age of 15 Myr, a reddening $E(B-V) = 1.1$ and a corrected distance modulus $(m-M)_0 = 11.70$.

As for the other two clusters (Ruprecht 10 and Haffner 7), no studies exist in the literature to our knowledge.

3 CLUSTER EXISTENCE AND NATURE

Before entering into the details of the data analysis, a word of caution is in order. We are here dealing with poor stellar groups, as can be seen in the CCD images in Fig. 1. Following Platais, Kozhurina-Platais & van Leeuwen (1998), we define as a physical group or a gravitationally bound system (at odd with a random sample of field stars), an ensemble of stars which (1) occupy a limited volume of space, (2) individually share a common space velocity, and (3) individually share the same age and chemical composition, producing distinctive sequence(s) in the Hertzsprung–Russell (HR) diagram.

Unfortunately, we do not have kinematic information for these objects, and therefore we are going to rely on the HR diagram and star density profiles for deciding on the nature and existence of these six stellar systems.

We start with CCD images to see what the clusters look like. By inspecting Fig. 1 closely, we note that all of them stand above the field, and fall close to the centre of the Y4KCAM mosaic using catalogued coordinates (Dias et al. 2002). The only exception is Haffner 7 (mid-right image in Fig. 1) which we were forced to position in the upper left-hand corner of the detector to avoid the

[5] http://www.univie.ac.at/webda/navigation.html

Table 3. A sample of the available photometric data for the star cluster Haffner 4. 99.9999 values are for not available measures.

ID	RA (°)	Dec. (°)	U (mag)	σ_U (mag)	B (mag)	σ_B (mag)	V (mag)	σ_V (mag)	I (mag)	σ_I (mag)
1	106.3883529	−14.8720246	9.4054	0.0173	9.9289	0.1974	7.4300	0.0318	6.2286	0.0555
2	106.5810012	−14.9762229	9.2274	0.0154	9.3976	0.0157	9.2511	0.0161	9.0499	0.0516
3	106.4797390	−15.0037127	10.5342	0.0124	99.9439	99.9999	99.9999	99.9999	99.9999	99.9999
4	106.4823592	−14.9494247	10.4104	0.0119	10.5902	0.0112	10.5082	0.0114	10.3128	0.0510
5	106.4901779	−14.8493842	99.9999	99.9999	99.9999	99.9999	99.9999	99.9990	8.8061	0.0534
6	106.4469765	−14.9727220	11.2471	0.0136	11.2699	0.0120	10.7533	0.0119	10.0105	0.0512
7	106.5754512	−15.0452087	11.5660	0.0125	11.4621	0.0123	11.1297	0.0115	10.6893	0.0514
8	106.6732766	−14.8446577	12.4649	0.0218	13.3356	0.2078	10.2985	0.0329	9.1951	0.0673
9	106.5506869	−14.9631866	11.8655	0.0123	11.8413	0.0121	11.3144	0.0118	10.6159	0.0510
10	106.5745932	−14.9484442	12.0282	0.0144	11.9441	0.0129	11.3918	0.0129	10.6919	0.0510

$V = 2.40$ mag η Canis Major variable star, which happens to fall less than 10 arcmin from Haffner 7 centre. All the clusters exhibit low density against the field, which seems to indicated that they are low mass, sparse objects on the verge of dissolving into the general Galactic field.

We performed star counts on the photometric data sets to derive an estimate of clusters' radial extents. These have been calculated following the same procedure described in Seleznev et al. (2010) and Carraro & Costa (2007).

Star counts and density contour maps (see Figs 3 and 4) confirm the visual impression of CCD images, and indeed the density of stars in the cluster's area goes from only two to five times the density in the surrounding fields, as measured away from the clusters' area (see Janes & Hoq 2011 for a similar situation). Looking at the right-hand columns, where the radial density profiles are shown, one can appreciate how the clusters are in fact small, with radii of the order of 2–3 arcmin only. The radius has been taken at the point where star counts reach the field level, as measured in the field far away from the cluster. The adopted radii are listed in Table 4, together with the basic parameters inferred in the next sections. They are in agreement with the visual estimates reported in Dias et al. (2002).

We therefore conclude that all these clusters are indeed made of groups of stars spatially concentrated and standing above the general Galactic field.

Besides, looking at the middle panels of Fig. 3, where contour maps are presented, one can see how the two-dimensional structure of these clusters is far from spherical. They show elongated shapes, stretched in one or more directions and, in some cases, with more than one density peak in the cluster area. We are tempted to interpret these complicated structures as evidence that the clusters are undergoing dissolution due to the interaction with the Galactic environment. The ages we find for them, larger than 1 Gyr (see next sections), confirm this fact, since the typical lifetime for a Galactic cluster in the Milky Way is around 200 million years (Wielen 1971; Pavani & Bica 2007). The only exception – and a confirmation of this scenario – is the younger cluster Haffner 15, which looks clearly spherical. We stress, anyway, that these are qualitative conclusions driven by the photometric data only, and that a dynamical study employing radial velocities of individual stars can more firmly assess the dynamical status of these poor systems.

4 COLOUR–MAGNITUDE DIAGRAMS OF CLUSTERS AND SURROUNDING FIELDS

In Figs 4 and 5, we present the colour–magnitude diagram (CMD) and colour–colour diagram (CCD) of the regions containing the six clusters under study. Only stars having photometric errors lower than 0.05 mag in all the four filters are plotted. In a wide field as the one we used (20 arcmin on a side) none of the clusters clearly emerges from the field in the CMDs, except for Haffner 15 (upper row in Fig. 6). All the clusters are hidden inside a rich field star population. The latter shows the typical features of any stellar field projected towards the Canis Major overdensity, namely a *blue plume* of young stars and a prominent blue faint sequence which runs to the left of the nearby stars main sequence (MS) and crosses it at $16.5 \leq V \leq 18.5$, depending on the field. These features have been described and extensively interpreted e.g. in Carraro et al. (2008, 2010), to which we refer the reader for further details.

The aim of this paper instead is to derive the fundamental parameters of these six clusters, and for this reason we are going to extract photometry only for those stars which fall inside the cluster radius, as estimated in Section 1.5. This will have the effect of alleviating the field star contamination, which we expect to be significant since these lines of sight (see Table 1) are projected towards the warped thin disc (Carraro et al. 2008).

We are not going to present any statistical cleaning of the clusters' CMD, since the number statistics in this clusters' sample is poor, and would generate artificial clumps and voids, which are difficult to be removed, and would complicate the interpretation of the diagrams. In the series of Figs 7–12, we present the CMD of each cluster and two realizations of the surrounding field, with the aim to highlight the cluster against the general field. This is possible thanks to the small size of the clusters and the wide field of our observations. In each of Figs 6–11, the cluster CMD (lower left-hand panel) is constructed by considering all the stars falling inside a circle whose radius is close to the cluster radius, as estimated in Section 3. The corresponding area in the cluster map is shown in the upper left-hand panel.

We then constructed CMDs for two different regions outside the cluster border, having about the same number of stars as the cluster region. In each figure the adopted radii are indicated together with the number of stars detected in each zone. In all cases the cluster region results to be significantly more populated than the corresponding field regions, which we needed to enlarge to include a comparable number of stars as in the cluster area.

Here below, we provide individual comments on a cluster-by-cluster basis.

Berkeley 76 (see Fig. 7). The CMD in the cluster region (left-hand panel) shows a conspicuous MS which suddenly drops at $V \sim 18.8$. The bluest point is at $V \sim 19.5$, which we consider as the MS turn-off point (TO). Another interesting feature is the compact group of four stars at $V \sim 17.9$ and $B - V \sim 1.4$, which does not have any

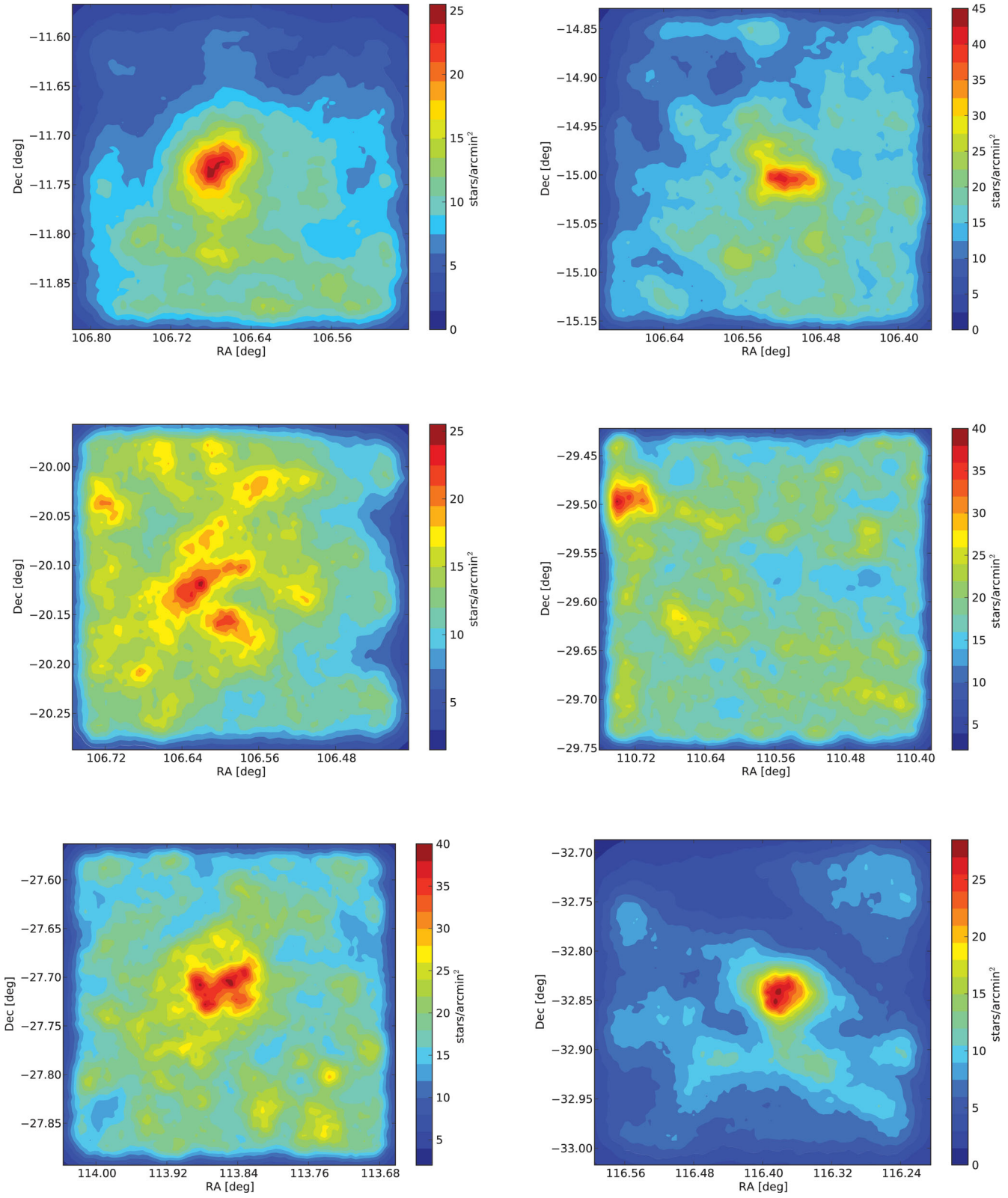

Figure 3. Contour density maps for the six clusters under study. Top row (from left to right): Berkeley 76 and Haffner 4; middle row (from left to right): Ruprecht 10 and Haffner 7; bottom row (from left to right): Haffner 11 and Haffner 15.

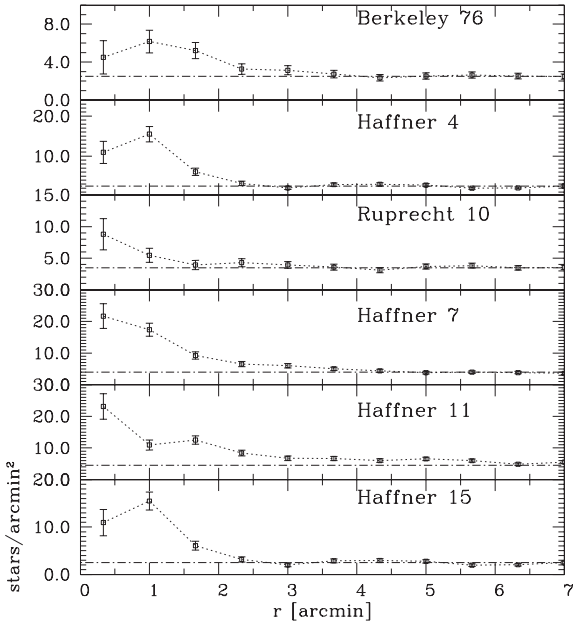

Figure 4. Radial density profiles for the six clusters under study.

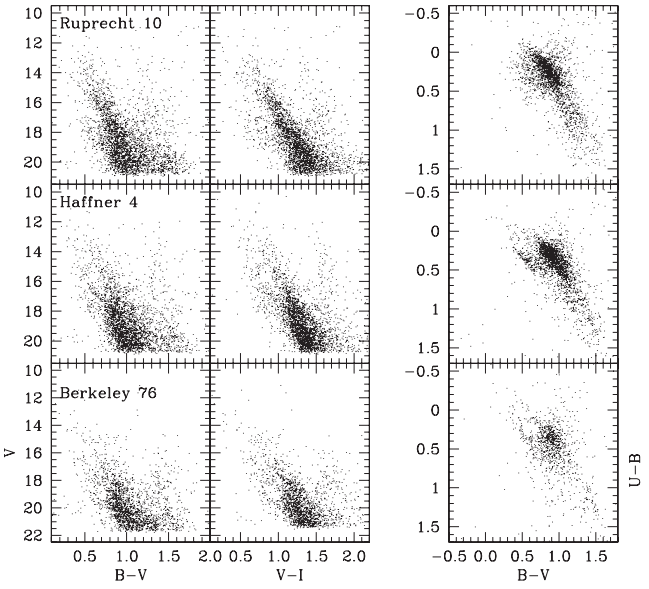

Figure 5. Colour–magnitude and colour–colour diagrams for Berkeley 76 (lower row), Haffner 4 (middle row) and Ruprecht 10 (upper row). Only stars having error in the all the passbands lower than 0.05 mag are shown.

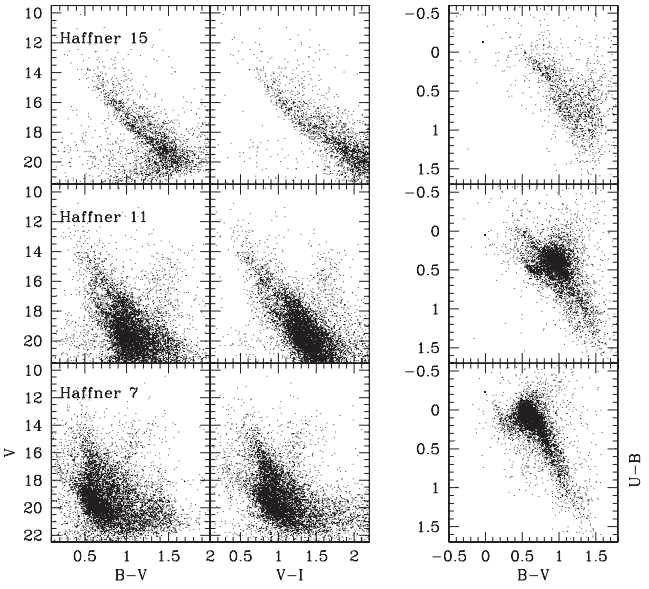

Figure 6. Colour–magnitude and colour–colour diagrams for Haffner 7 (lower row), Haffner 11 (middle row) and Haffner 15 (upper row). Only stars having error in all the passband lower than 0.05 mag are shown.

counterpart in the field, as indicated by the red box circumscribing it. These stars are plotted as red dots in the corresponding map. Their position inside the cluster region lends further support to their identification as red clump stars members to the cluster. We are going to consider this as the cluster red giant branch (RGB) clump. We believe that this set of CMDs convincingly shows that we are facing a real star cluster. We shall derive estimates of its basic parameters in the next section.

Haffner 4 (see Fig. 8). Also in this case the cluster CMD reveals an MS significantly more populated than in the field star CMDs. It is difficult to say where the TO is located, but we tentatively identify it at $V \sim 15.0$ and $B - V \sim 0.5$. We do see a possible trace of a RGB clump in the star that we enclosed in the red box. Two redder stars can be part of the RGB as well. This star is plotted as a red dot in the corresponding map. Its position inside the cluster region lends further support to its identification as red clump star member to the cluster. We shall derive estimates of its basic parameters in the next section.

Ruprecht 10 (see Fig. 9). The interpretation of Ruprecht 10 CMD is not straightforward at all. We tentatively consider as the MS the bright sequence terminating at $V \sim 14$ and $B - V \sim 0.3$, while the vertical sequence terminating at $V \sim 18.5$ is produced by field stars, since it is visible also in the field star CMDs. Moreover, we

Table 4. Fundamental parameters estimated for the clusters. $d_\odot$ indicates the distance of a cluster from the Sun, Z indicates the height below the Galactic plane and R_{GC} indicates its distance to the Galactic centre.

Name	Radius (arcmin)	$E(B-V)$ (mag)	$(m-M)_V$ (mag)	$d_\odot$ (kpc)	Age (Gyr)	Z (pc)	R_{GC} (kpc)
Berkeley 76	2.5 ± 0.5	0.55 ± 0.10	17.20 ± 0.15	12.6	~ 1.5	~ -0.45	~ 17.4
Haffner 4	2.5 ± 0.5	0.50 ± 0.10	14.80 ± 0.15	4.5	~ 0.5	~ -0.28	~ 11.9
Ruprecht 10	2.0 ± 0.5	0.38 ± 0.10	13.40 ± 0.15	2.9	~ 1.1	~ -0.30	~ 10.5
Haffner 7	1.5 ± 0.5	0.13 ± 0.10	13.65 ± 0.15	4.5	~ 1.5	~ -0.50	~ 11.3
Haffner 11	2.0 ± 0.5	0.32 ± 0.05	14.90 ± 0.10	6.0	~ 0.8	~ -0.40	~ 12.5
Haffner 15	2.0 ± 0.5	1.05 ± 0.25	16.00 ± 0.10	3.5	~ 0.02	~ -0.25	~ 10.3

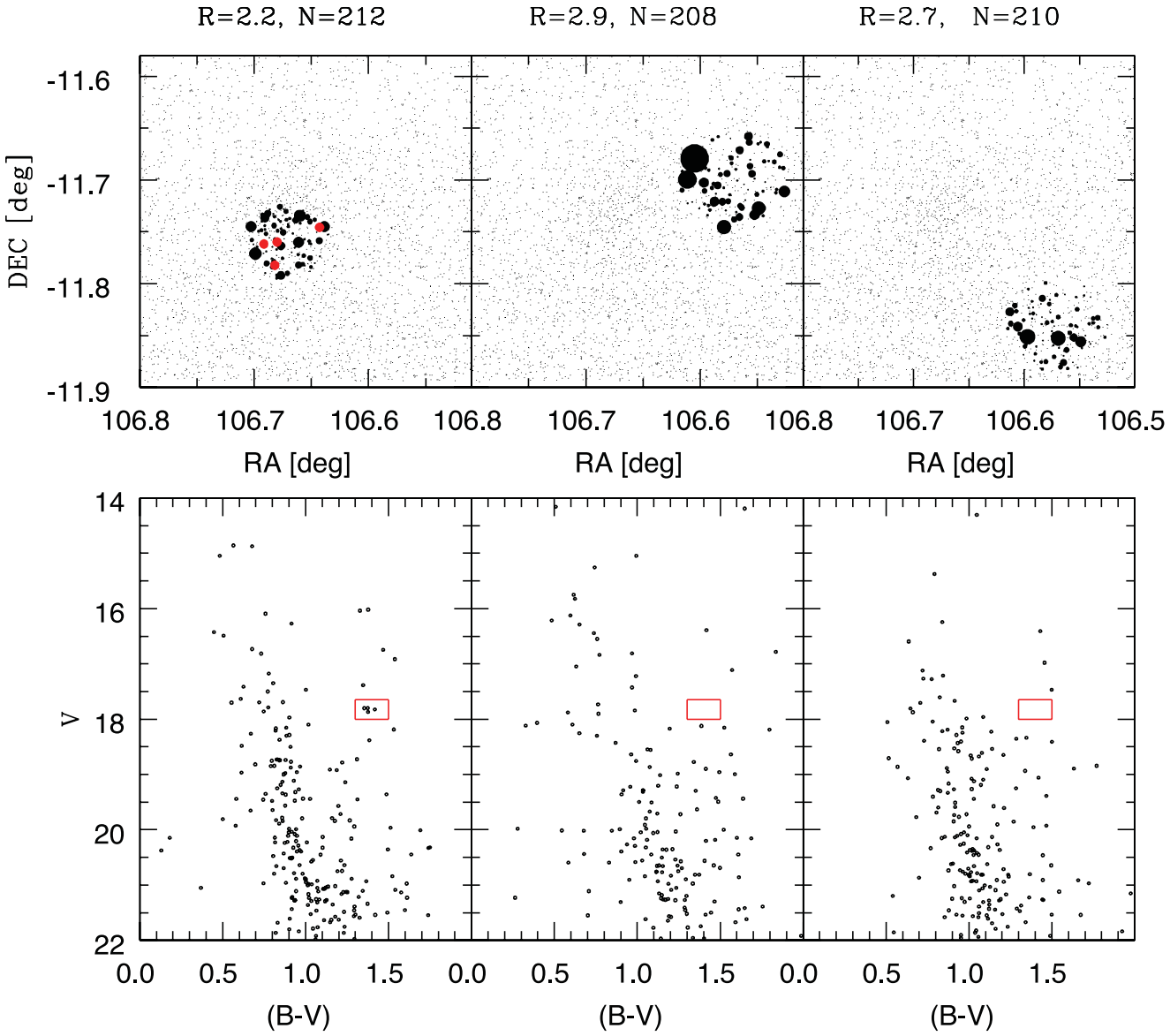

Figure 7. CMDs of Berkeley 76 and surrounding fields. Stars inside these regions are plotted with symbols proportional to their magnitude. The red box indicates the position of clump stars. These stars are plotted as red filled circles in the corresponding map.

consider as clump stars the two stars at $V \sim 14$ and $B - V \sim 1.4$. These stars are plotted as red dots in the corresponding map. Their position inside the cluster region lends further support to their identification as red clump stars members to the cluster. We are going to provide estimates of the fundamental parameters in the next section.

Haffner 7 (see Fig. 10). This is by far the most complicated object, because we could not cover it completely, as discussed in Section 3. The cluster CMD looks different from the field CMDs, and shows a clear MS. The bluest point is at $V \sim 16.50$, which we consider as the MS TO. Another interesting feature is the sparse group of four stars at $V \sim 14.5$ and $B - V \sim 1.1$, which does not have any counterpart in the field, as indicated by the red box circumscribing it. These stars are plotted as red dots in the corresponding map. Their position inside the cluster region lends further support to their identification as red clump stars members to the cluster. We conclude that in the region of Haffner 7 there is a star concentration, and this concentration shows distinctive features in the CMD. We are going to provide estimates of the fundamental parameters in the next section.

Haffner 11 (see Fig. 11). This is undoubtedly a nice intermediate-age cluster, with a conspicuous clump of stars (enclosed in a red box) at $V \sim 16$ and $B - V \sim 1.3$. These stars are plotted as red dots in the corresponding map. Their position inside the cluster region lends further support to their identification as red clump stars members to the cluster. The MS TO is located at $V \sim 16.5$. The vertical sequence which drops at $V \sim 16.5$ redwards of the cluster MS is produced by the field, and appears also in the field star CMDs. Haffner 11 is the most obvious cluster amongst the ones discussed so far.

Haffner 15 (see Fig. 12). From the appearance of the cluster area CMD we infer that Haffner 15 is a young cluster, with a TO at $V \sim 15.5$ and no indication of RGB stars. The MS is prominent and much more populated than in the field star CMDs, where the typical vertical sequence from the disc is visible. The colour of the TO indicates that the cluster is significantly reddened. We are

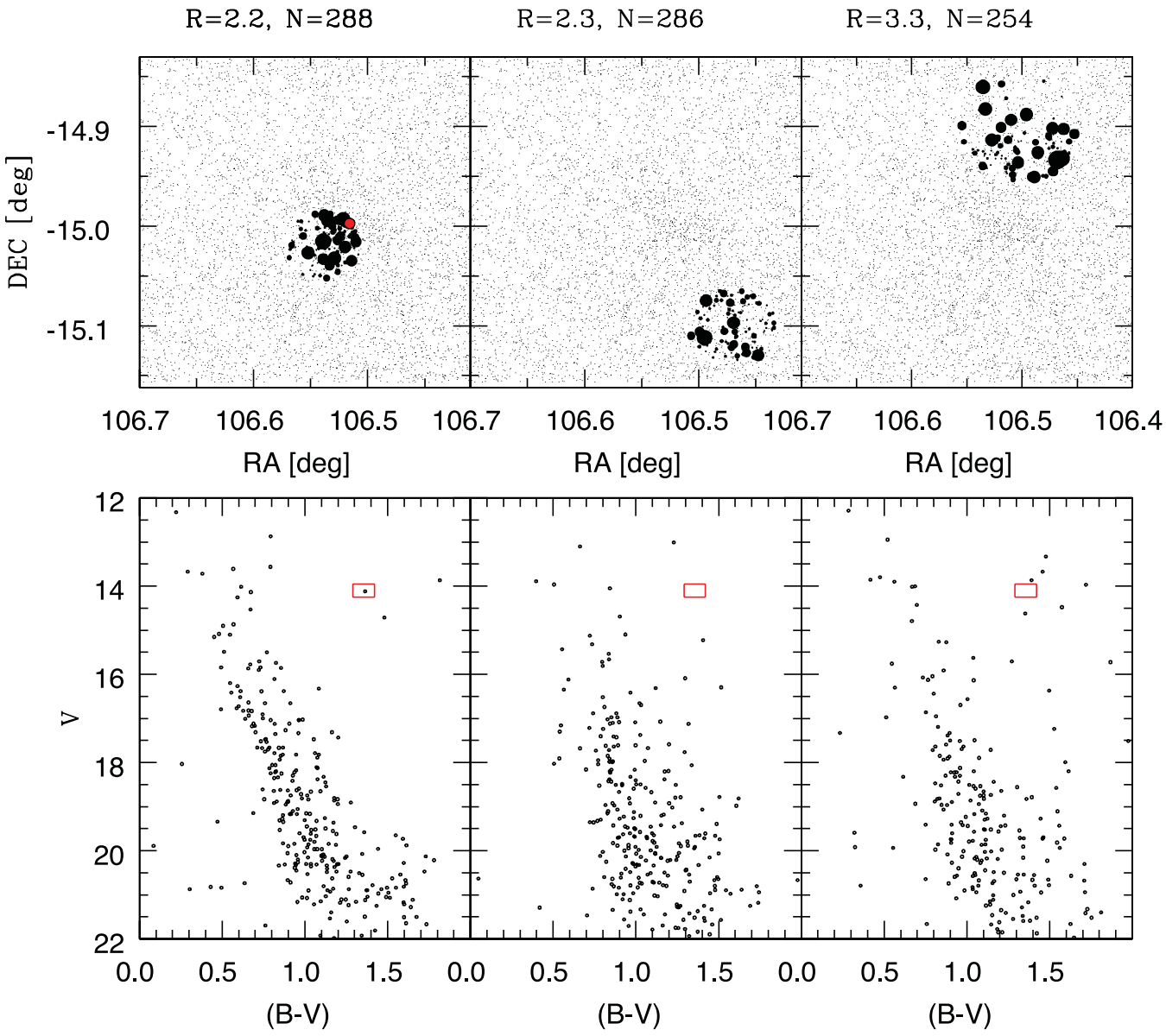

Figure 8. CMDs of Haffner 4 and surrounding fields. Stars inside these regions are plotted with symbols proportional to their magnitude. The red box indicates the position of clump stars. These stars are plotted as red filled circles in the corresponding map.

going to provide estimates of the fundamental parameters in the next section.

5 DERIVATION OF CLUSTERS' BASIC PARAMETERS

The CMDs generated with only the cluster region (as defined in Section 1.5) stars are here compared with isochrones extracted from the Padova suite of models (Marigo et al. 2008). This allows us to infer estimates of clusters age, distance and reddening, by assuming conservative values of the metallicity. We are fully aware that this process is highly subjective, and for this reason we consider the values we obtain as estimates, awaiting studies which can provide measures of the clusters' metal abundance.

In fact, we are here facing the well-known problem of associating reliable errors to distance and age. Without precise estimates of reddening and metallicity, it is extremely difficult to perform a proper error assessment. In theory this would imply a full error propagation which would in general produce a very large hypervolume in the parameters' space with many solutions which would not pass a simple by-eye inspection.

We will, therefore, limit ourselves to provide fitting errors for the cluster reddening and apparent distance moduli, being totally aware that they most probably are only rough lower limits awaiting improvements as soon as more precise metallicity measurements will be available. However, in deriving distance, a full propagation is done taking into account the whole range of values for reddening and distance modulus. Finally, as far as the ages are concerned, only fitting errors are reported, adopting solar metallicity (see below).

For consistency with previous studies we shall adopt 8.5 kpc as the Sun distance to the Galactic centre, and 3.1 for the ratio of total to selective absorption $R_V = \frac{A_V}{E(B-V)}$, which Moitinho (2001) demonstrated to be of general validity in this Milky Way sector.

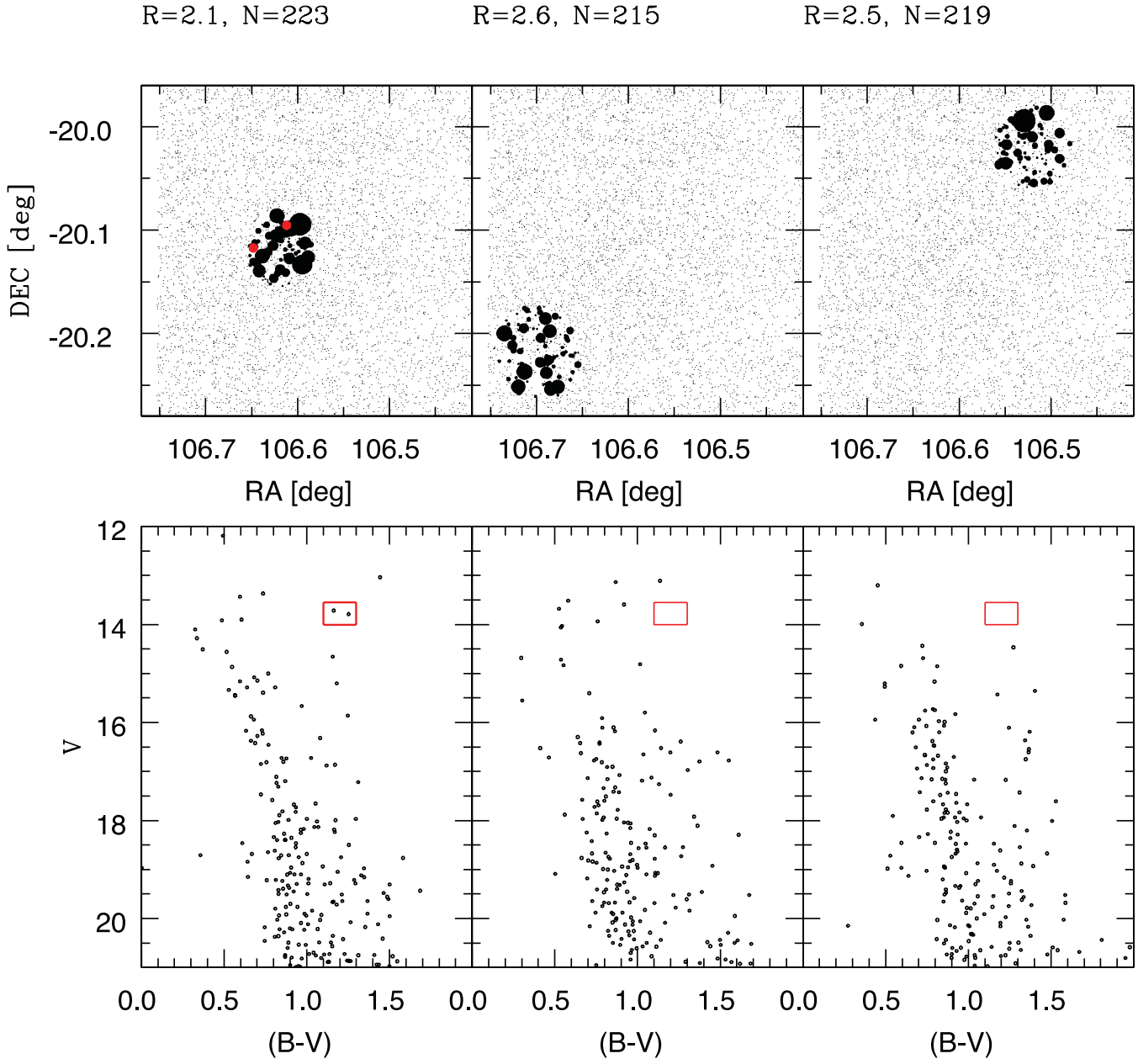

Figure 9. CMDs of Ruprecht 10 and surrounding fields. Stars inside these regions are plotted with symbols proportional to their magnitude. The red box indicates the position of clump stars. These stars are plotted as red filled circles in the corresponding map.

Berkeley 76 (see Fig. 13). The CMDs for this cluster have been derived plotting all the stars within 2.5 arcmin from the cluster centre. Still the contamination is significant, and makes the exercise of fitting an isochrone quite challenging. As previously discussed, we consider as cluster RGB clump the group of four stars at $V \sim 17.85$ and $(B - V) \sim 1.35$. Such a small number of clump stars are not unusual in old open clusters, as one can see also in very recent studies (e.g. King 8 or Berkeley 23; Cignoni et al. 2011). The TO is located at $V \sim 19.5$ and $(B - V) \sim 0.85$.

If we use this interpretation of the cluster CMD, we end up with an age of about 1.5 Gyr. The overimposed – half-solar ($Z = 0.008$) – isochrone fits also the slope and shape of the MS. The mismatch in colour for the clump is of the order of $\Delta(B - V) \sim 0.08$ mag, and can be due to a variety of reasons, like colour transformations and/or mixing length calibration issues (see Palmieri et al. 2002; Carraro & Costa 2007). We also tried solar metallicity, which does not seem suitable for an outer disc cluster, and found that, for a comparable age, the fit to the MS is acceptable, but the mismatch in colour with the cluster clump is much more severe.

For the adopted age and metallicity, Berkeley 76 has a reddening $E(B - V) = 0.55 \pm 0.1$ [$E(V - I) = 0.75 \pm 0.10$] and a distance modulus $(m - M)_V = 17.15 \pm 0.20$. Uncertainties in reddening and distance have been estimated by eye, shifting the isochrone along the horizontal and vertical directions, respectively, and estimating the range of values that yield acceptable fits. As a consequence, the heliocentric distance is 12.6 kpc, and the distance from the Galactic centre is 17.4 kpc, making this cluster one of the most peripheral old open cluster in the outer disc (Carraro et al. 2007a).

These results are in basic agreement with Hasegawa et al. (2008), except for the distance. Looking at their results (their fig. 2) for

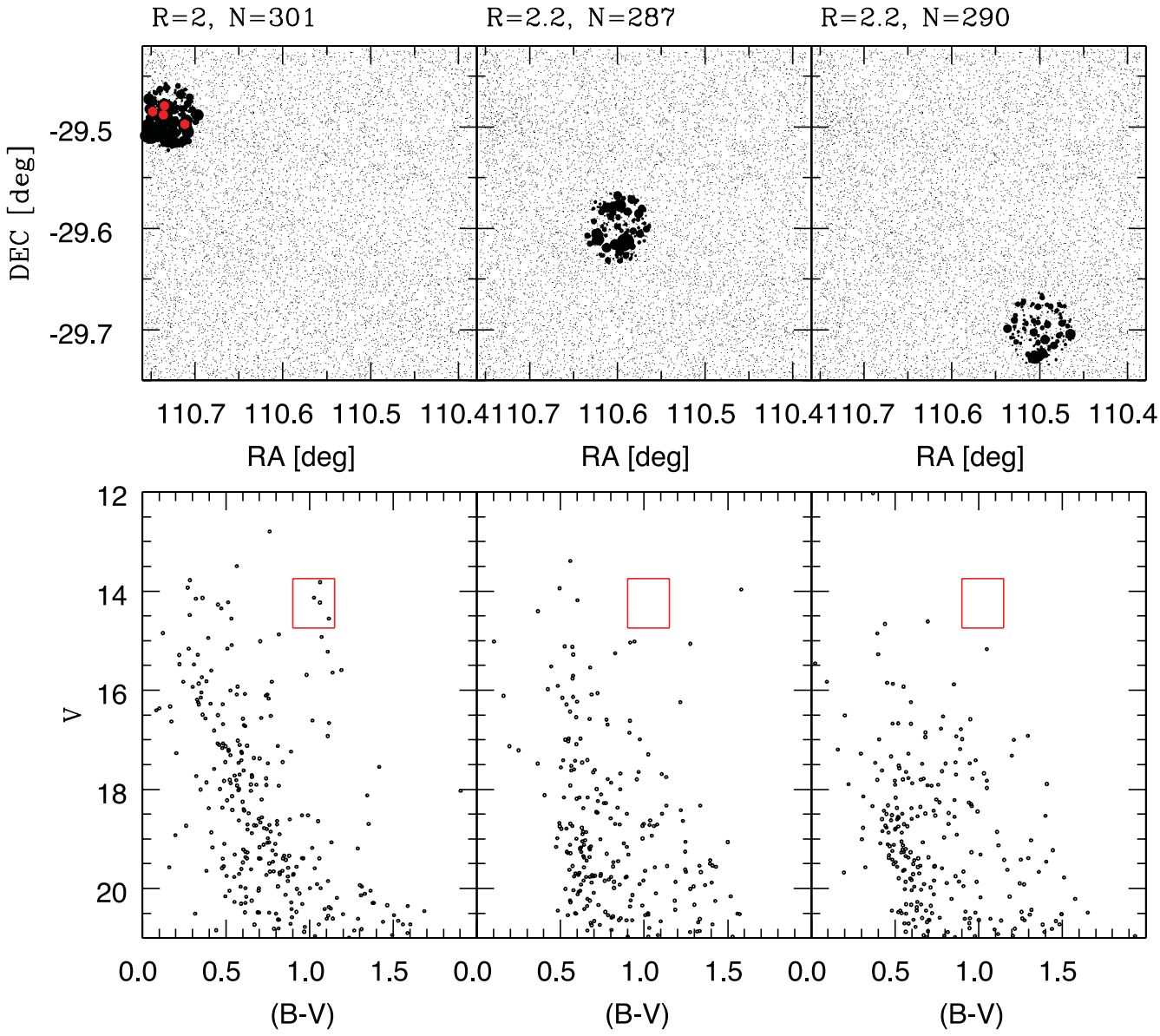

Figure 10. CMDs of Haffner 7 and surrounding fields. Stars inside these regions are plotted with symbols proportional to their magnitude. The red box indicates the position of clump stars. These stars are plotted as red filled circles in the corresponding map.

Berkeley 76, one can indeed note that the fit to the magnitude of the red clump is offset by almost half a magnitude, with the isochrone clump being too bright. This explains, in turn, the smaller distance in their study.

Haffner 4 (see Fig. 14). As for the previous cluster, we selected only the stars inside the cluster radius (see Table 4). In this case we use solar metallicity isochrones, since the cluster is presumably located closer than Berkeley 76. Haffner 4 looks scarcely populated, and severely contaminated by field stars. The best-fitting isochrone is for an age of 0.5 Gyr, which nicely follows the shape of the MS and the TO curvature, at $V \sim 15.0$ and $(B - V) \sim 0.5$. No obvious indications of a red clump are present. The fit shown in Fig. 7 yields a reddening $E(B - V) = 0.50 \pm 0.10$ [$E(V - I) = 0.63 \pm 0.10$] and a distance modulus $(m - M)_V = 14.80 \pm 0.15$. Once corrected, this implies a distance from the Sun of 4.4 kpc, and of 11.9 kpc from the Galactic centre.

In this case our results imply an age lower than the one suggested by Hasegawa et al. (2008), and a solar metallicity.

Ruprecht 10 (see Fig. 15). This cluster is sparse and has quite a distorted shape, which might indicate a stage of advanced disgregation. The MS and the evolved region of the CMD are scarcely populated. The TO is located at $V \sim 15.0$ and $(B - V) \sim 0.5$, and the clump at $V \sim 14.0$ and $(B - V) \sim 1.25$. By considering the stars within the cluster estimated radius, we obtained an acceptable fit for a half-solar metallicity isochrone of 1.1 Gyr, as shown in Fig. 8. This fit provides a reddening $E(B - V) = 0.28 \pm 0.10$ and a distance modulus $(m - M)_V = 13.40 \pm 0.10$. This, in turn, yields a heliocentric distance of 2.9 kpc, and a distance from the Galactic centre of 10.5 kpc.

Haffner 7 (see Fig. 16). The TO is located at $V \sim 16.0$ and $(B - V) \sim 0.70$, and the clump at $V \sim 14.5$ and $(B - V) \sim 1.5$. By considering the stars within the cluster estimated radius, we

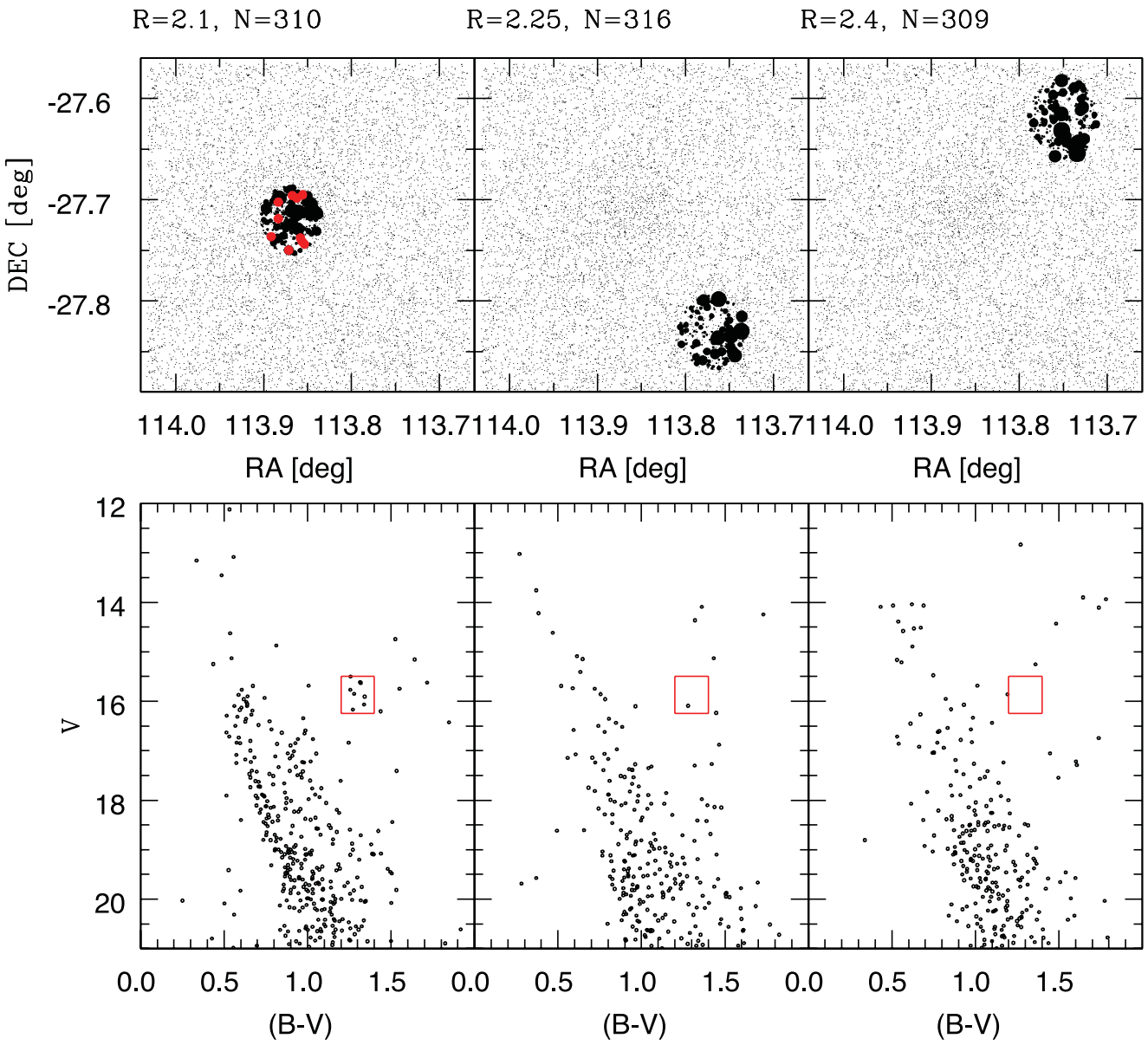

Figure 11. CMDs of Haffner 11 and surrounding fields. Stars inside these regions are plotted with symbols proportional to their magnitude. The red box indicates the position of clump stars. These stars are plotted as red filled circles in the corresponding map.

obtained an acceptable fit for a half-solar metallicity isochrone of 1.5 Gyr, as shown in Fig. 8. This fit provides a reddening $E(B-V) = 0.13 \pm 0.10$ and a distance modulus $(m-M)_V = 13.65 \pm 0.10$. This, in turn, yields an heliocentric distance of 4.5 kpc, and a distance from the Galactic centre of 11.3 kpc.

Haffner 11 (see Fig. 17). This cluster results to be a nice intermediate-age open cluster, with a well-defined clump and not much contamination, when stars inside the cluster radius are isolated, and in agreement with all previous studies. It was quite an easy tasks to super-impose on the cluster sequence a solar metallicity isochrone for an age of 800 million years, which yields a good fit in both the CMDs. From this fit we derive a reddening $E(B-V) = 0.35 \pm 0.05$ and an apparent distance modulus $(m-M)_V = 15.0 \pm 0.10$. We therefore place the cluster at 6.0 kpc from the Sun, and 12.5 kpc from the Galactic centre.

Our results are therefore closer to Bica & Bonatto (2005) than to Piatti et al. (2009).

Haffner 15 (see Figs 18 and 19). The preliminary estimate of the age of Haffner 15 in Vázquez et al. (2008) was 600 million years, significantly larger than the 15 Myr reported by Paunzen et al. (2006). To solve this discrepancy we make use of a different set of diagrams. In detail, we make first use of the $U-B/B-V$ CCD, which is shown in Fig. 18. Here the solid line is an empirical zero-age MS (ZAMS) from Schmidt-Kaler (1982). The same ZAMS (dashed line) is shifted by $E(B-V) = 1.05$ along the reddening vector (indicated by the arrow in the plot) to fit the bulk of Haffner 15 stars. As justified above, we adopted a normal reddening law, which implies $R_V = 3.1$ and $E(U-B)/E(B-V) = 0.72$. To guide the eye, a few relevant spectral types are indicated, together with their displacement along the reddening path.

As a result, the cluster reddening is $E(B-V) = 1.05 \pm 0.25$, and the large dispersion indicates that the cluster suffers from significant variable reddening.

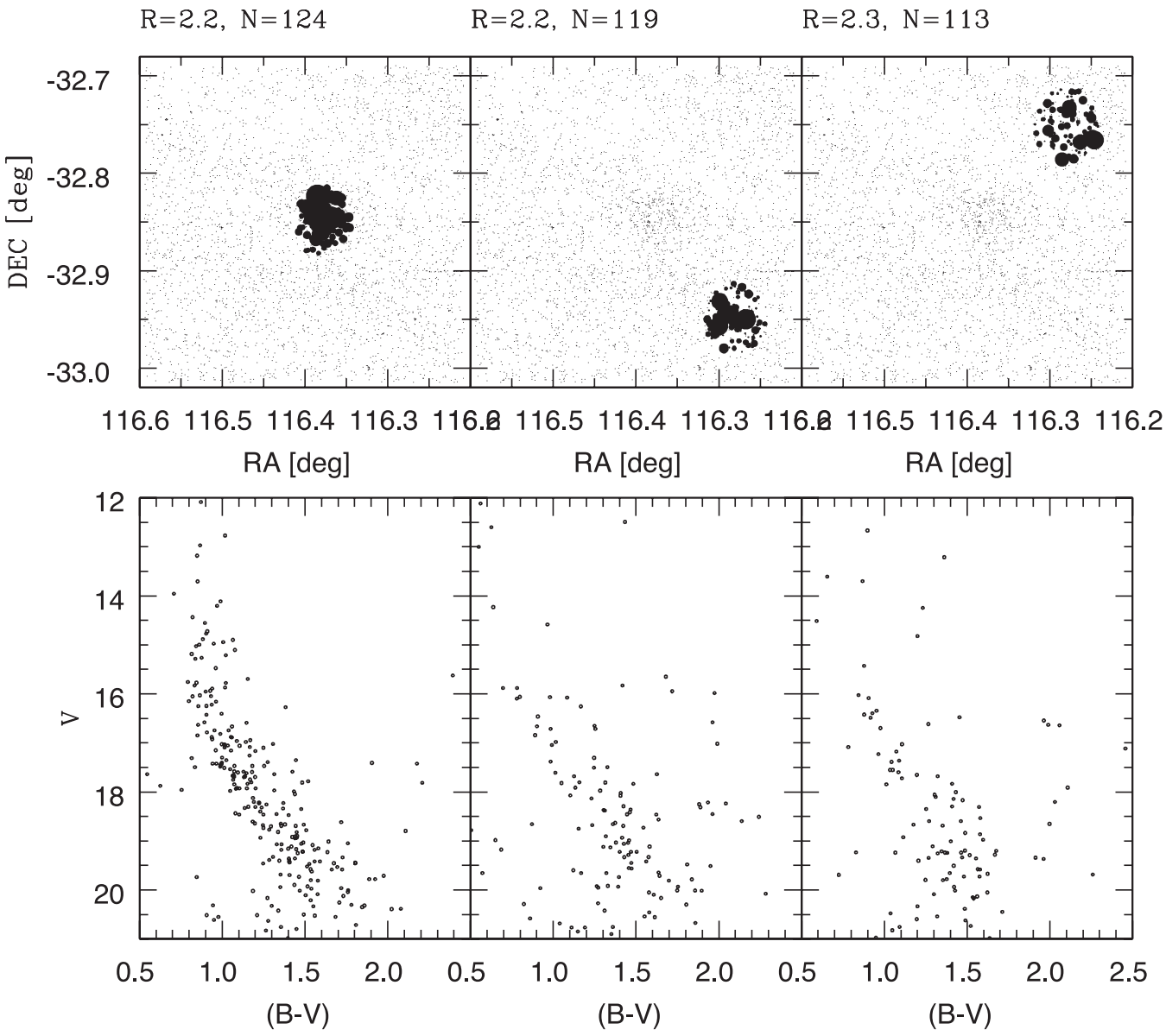

Figure 12. CMDs of Haffner 15 and surrounding fields. Stars inside these regions are plotted with symbols proportional to their magnitude.

We now make use of the Q method (Strayzis 1991; Carraro et al. 2010) to derive individual stars reddening, and from them compute their absolute magnitude and colours. These values are then used to build up the reddening-corrected CMDs in Fig. 19, in the $(B-V)_o$ versus V_o plane (left-hand panel), and in the $(U-B)_o$ versus V_o plane (right-hand panel). We super-pose to the star distribution the same empirical ZAMS used before. Here the only free parameter is the distance modulus, which turns out to be $V_o - M_V = 13.00 \pm 0.10$, in both diagrams. One can better appreciate the fit in the $(U-B)_o$ versus V_o CMD, since the MS is more tilted in this diagram. The TO point is located at $V_o \sim 11.50$ ($V \sim 14.5$), which translates into $M_V = -1.50$. This means that the stars leaving the MS are of approximate spectral type B2, as confirmed also by inspecting the two colour diagrams in Fig. 11. As a consequence, one can estimate the cluster age to be around 10–20 million years (Marigo et al. 2008).

The apparent distance modulus $(m - M)_V$ is then 16.0 ± 0.10. Overall, we therefore confirm Paunzen et al. (2006) results that Haffner 15 is indeed a young, extremely reddened open cluster. It is located 3.5 kpc from the Sun, and 10.3 kpc from the Galactic centre. Such distance is compatible with Haffner 15 membership to the Perseus arm, or to the local (Orion) arm extension in the third Galactic quadrant (Levine, Blitz & Heiles 2006; Moitinho et al. 2006; Vázquez et al. 2008).

6 DISCUSSION AND CONCLUSIONS

We have presented and discussed *UBVI* CCD photometry of six Galactic star clusters projected against the Canis Major overdensity in the third quadrant of the Milky Way: Berkeley 76, Haffner 4, Ruprecht 10, Haffner 7, Haffner 11 and Haffner 15. The fields they are immersed in have already been analysed in Vázquez et al. (2008), where we searched for young diffuse stellar populations to be used as tracers of the spiral structures of the outer disc. Here we concentrated on the clusters themselves, with the goal of deriving estimates of their age and distance.

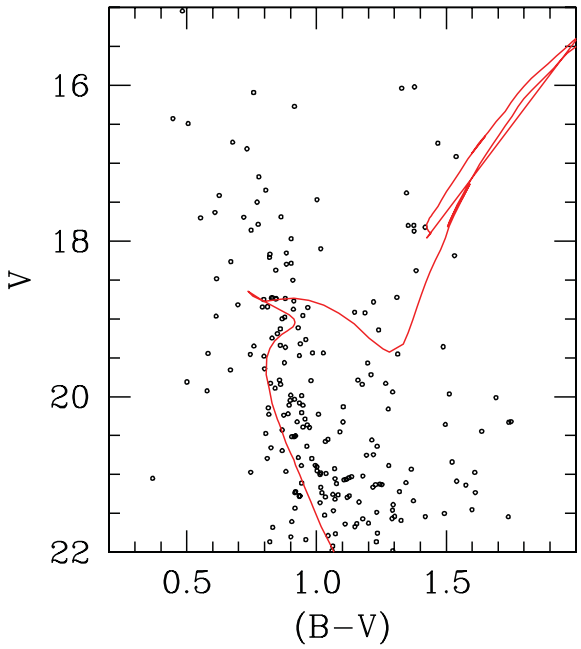

Figure 13. Isochrone solution for Berkeley 76 in the $V/B-V$ CMD. Fitting parameters are summarized in Table 4.

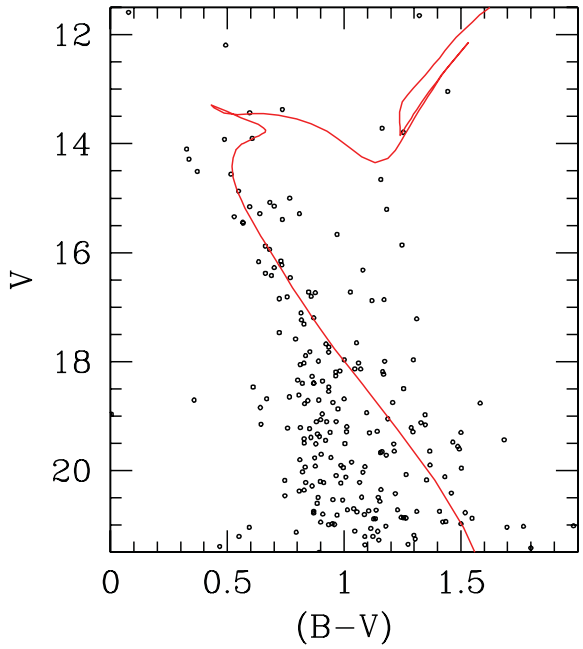

Figure 15. Isochrone solution for Ruprecht 10 in the $V/B-V$ CMD. Fitting parameters are summarized in Table 4.

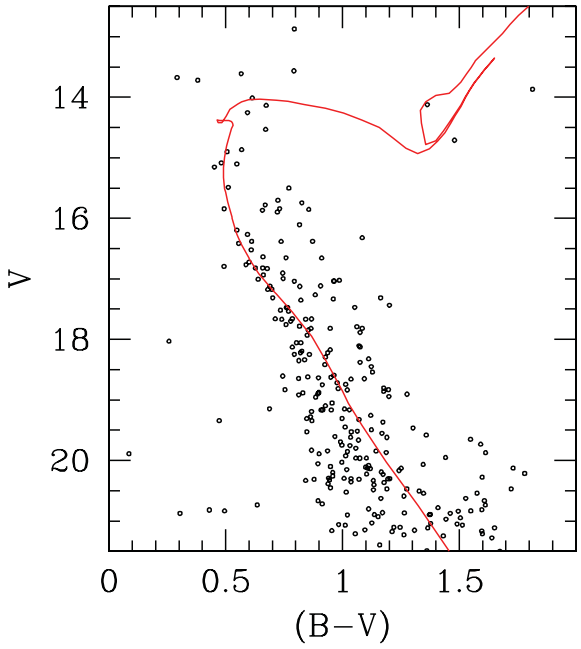

Figure 14. Isochrone solution for Haffner 4 in the $V/B-V$ CMD. Fitting parameters are summarized in Table 4.

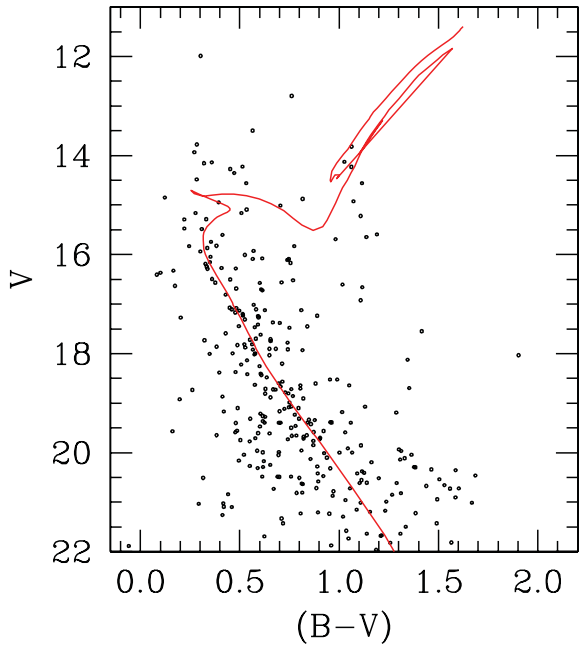

Figure 16. Isochrone solution for Haffner 7 in the $V/B-V$ CMD. Fitting parameters are summarized in Table 4.

We can summarize our results as follows (see also Table 4).

(i) According to star counts, all the objects appear as significant overdensities with respect to the field.

(ii) The cluster Haffner 15 is the only young object of the sample. For its age and distance it is a probable member of the Perseus arm or of the extension of the local arm into the third Galactic quadrant. This cluster is heavily and differentially reddened.

(iii) We found one old star cluster at the extreme periphery of the disc, at a mean distance of more than 17 kpc from the Galactic centre: Berkeley 76; only Saurer 1 and Berkeley 29 are located further than them (Carraro & Baume 2003).

(iv) Ruprecht 10 and Haffner 7, two clusters that were never studied before, are found to have ages larger than 1 Gyr.

(v) The spatial shape of these clusters, as highlighted with star counts, may witness their dynamical status. Haffner 15, the youngest, has an almost two-dimensional circular shape, while all the others – older than the Hyades – have complicated structures, very far from spherical. We suggest that they are close to dissolution and merging with the general Galactic field, although their

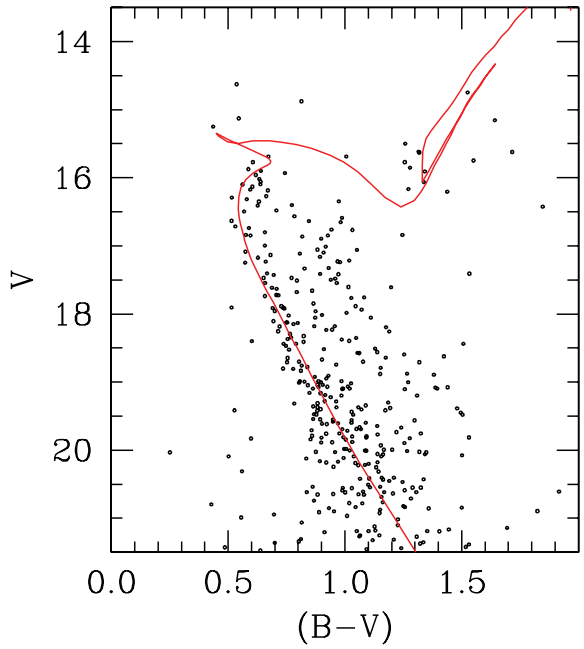

Figure 17. Isochrone solution for Haffner 11 in the $V/B-V$ CMD. Fitting parameters are summarized in Table 4.

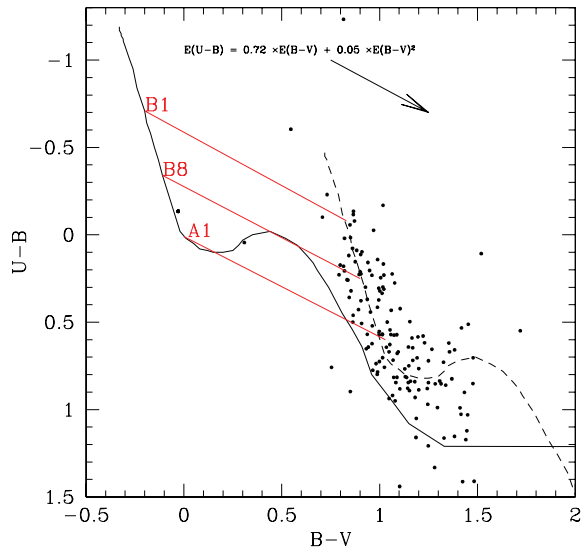

Figure 18. Two colour diagrams for Haffner 15. Only stars falling inside the cluster radius are plotted. The solid line is an empirical unreddened ZAMS. The same ZAMS, shifted by $E(B-V) = 1.05$ along the reddening path, is shown with a dashed line. The reddening vector for a normal reddening law is indicated with an arrow. To guide the eye, a few relevant spectral types are also indicated along the zero reddening ZAMS, together with their displacement along the reddening vector direction.

actual dynamical status can only be confirmed with individual stars kinematics.

We believe that this sample of clusters is quite promising, and deserves a much closer look in the future, which unfortunately *Gaia* will not be able to provide at those distances. The oldest, most distant clusters, in particular, are excellent targets to further probe the slope of the abundance gradient in the outer disc, and its evolution with time (Twarog, Ashman & Anthony-Twarog 1997; Carraro et al. 2007; Magrini et al. 2009).

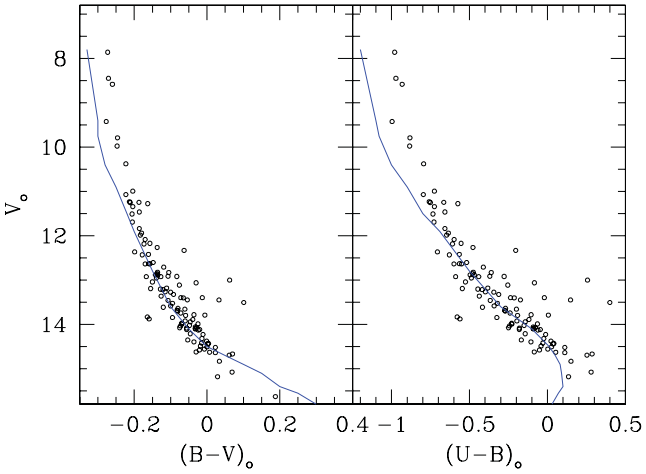

Figure 19. Reddening free CMDs in the $(B-V)$ versus V plane (left-hand panel) and $(U-B)$ versus V plane (right-hand panel). The solid line is a reddening free, empirical ZAMS shifted by $(V_o - M_V) = 13.00$.

ACKNOWLEDGMENTS

GC would like to mention and acknowledge the great support from Cerro Tololo Observatory staff, in particular from Edgardo Cosgrove. We thank warmly Sandy Strunk for reading the manuscript and helping us to improve the language. This study made use of the SIMBAD and WEBDA data bases.

REFERENCES

Bica E., Bonatto C., 2005, A&A, 443, 465
Carraro G., Baume G. L., 2003, MNRAS, 346, 18
Carraro G., Costa E., 2007, A&A, 464, 573
Carraro G., Maris M., Bertin D., Parisi M. G., 2006, A&A, 460, L39
Carraro G., Geisler D., Villanova S., Frinchaboy P. M., Majewski S. R., 2007a, A&A, 476, 217
Carraro G., Moitinho A., Zoccali M., Vázquez R. A., Baume G., 2007b, AJ, 133, 1058
Carraro G., Moitinho A., Vázquez R. A., 2008, MNRAS, 383, 1597
Carraro G., Vázquez R. A., Costa E., Perren G., Moitinho A., 2010, ApJ, 718, 683
Chou M.-Y., Majewski S. R., Cunha K., Smith V. V., Patterson R. J., Martínez-Delgado D., 2010, ApJ, 720, L5
Cignoni M., Beccari G., Bragaglia A., Tosi M., 2011, MNRAS, 416, 1077
Dias W. S., Alessi B. S., Moitinho A., Lépine J. R. D., 2002, A&A, 389, 871
Frinchaboy P. M., Majewski S. R., Crane J. D., Reid I. N., Rocha-Pinto J., Phelps R. L., Patterson R. J., Munoz R., 2004, ApJ, 620, L21
Hasegawa T., Sakamoto T., Malasan H. L., 2008, PASJ, 60, 1267
Janes K. A., Hoq S., 2011, AJ, 141, 92
Landolt A. U., 1992, AJ, 104, 340
Levine E. S., Blitz L., Heiles C., 2006, Sci, 312, 1773
López-Corredoira M., Momany Y., Zaggia S., Cabrera-Lavers A., 2007, A&A, 472, 47
López-Corredoira M., Moitinho A., Zaggia S., Momany Y., Carraro G., Hammersley P. L., Cabrera-Lavers A., Vazquez R. A., 2012, preprint (arXiv:1207.2749)
Magrini L., Sestito P., Randich S., Galli D., 2009, A&A, 494, 95
Marigo P., Girardi L., Bressan A., Groenewegen M. A. T., Silva L., Granato G. L., 2008, A&A, 482, 883
Moitinho A., 2001, A&A, 379, 476
Moitinho A., Vázquez R. A., Carraro G., Baume G., Giorgi E. E., Lyra W., 2006, MNRAS, 368, L77

Momany Y., Zaggia S., Gilmore G., Piotto G., Carraro G., Bedin L. R., de Angeli F., 2006, A&A, 451, 499
Palmieri R., Piotto G., Saviane I., Girardi L., Castellani V., 2002, A&A, 392, 115
Patat F., Carraro G., 2001, MNRAS, 325, 1591
Paunzen E., Nepotil M., Iliev I. Kh., Maitzen H. M., Claret A., Pintado O. I., 2006, A&A, 454, 171
Pavani D. B., Bica E., 2007, A&A, 468, 139
Piatti A. E., Clariá J. J., Parisi M. C., Ahumada A. V., 2009, New Astron., 14, 97
Platais I., Kozhurina-Platais V., van Leeuwen F., 1998, AJ, 116, 2423
Schlegel D. J., Finkbeiner D. P., Davis M., 1998, ApJ, 500, 525
Schmidt-Kaler Th., 1982, inSchaifers K., Voigt H. H., eds, Landolt-Börnstein, Numerical data and Functional Relationships in Science and Technology, New Series, Group VI, Vol. 2(b), Springer-Verlag, Berlin, p. 14
Seleznev A. F., Carraro G., Costa E., Loktin A. V., 2010, New Astron., 15, 61
Skrutskie M. F. et al., 2006, AJ, 131, 1163
Stetson P. B., 1987, PASP, 99, 191
Strayzis V., 1991, Multicolor Photometry, Astronomy and Astrophysics Series, Vol. 15
Twarog B. A., Ashman K. M., Anthony-Twarog B. J., 1997, AJ, 114, 2556
Vázquez R. A., May J., Carraro G., Bronfman L., Moitinho A., Baume G., 2008, ApJ, 672, 930
Wielen R., 1971, A&A, 13, 309

SUPPORTING INFORMATION

Additional Supporting Information may be found in the online version of this article:

Photometric data for the star clusters (http://mnras.oxfordjournals.org/lookup/suppl/doi:10.1093/mnras/sts038/-/DC1).

Please note: Oxford University Press are not responsible for the content or functionality of any supporting materials supplied by the authors. Any queries (other than missing material) should be directed to the corresponding author for the article.

This paper has been typeset from a TEX/LATEX file prepared by the author.